Steps toward Constructing a Cytochrome $b_6 f$ Complex in the Purple Bacterium *Rhodobacter Sphaeroides*: An Example of the Structural Plasticity of a Membrane Cytochrome†

Richard Kuras,*,‡ Mariana Guergova-Kuras,§ and Antony R. Crofts‡,§

Department of Microbiology and Center for Biophysics and Computational Biology, University of Illinois, Urbana, Illinois 61801

Received June 8, 1998; Revised Manuscript Received September 8, 1998

ABSTRACT: We have modified the cytochrome *b* subunit of the cytochrome bc_1 complex from the purple bacterium *Rhodobacter sphaeroides* to introduce two distinctive features of cytochrome $b_6 f$ complexes. In the first one, we have split cyt *b* into two polypeptides thus mimicking the organization of cyt b_6 and subunit IV in the $b_6 f$ complexes. In the second, an extra residue was added between His198 and Phe199, thus extending the span between the histidine ligands for the two *b*-hemes in helix D. The properties of the mutant strains were determined using thermodynamic and kinetic analysis. The two mutant enzymes were assembled and functioned so as to allow the photosynthetic growth of the mutant strains. For the split enzyme, we show that two independently translated fragments of cyt *b* are inserted in the membrane. Our results indicate a decrease in the stability of the semiquinone formed at the quinone reduction (Q_i) site in this mutant. This property, characteristic for $b_6 f$ complexes, indicates the functional importance of the connecting span between helices D and E. The presence of the inserted threonine in helix D modified the spectrum and redox potential of the b_L-heme, shifting the potential difference between the two *b*-hemes from 140 mV in the wild-type to 55 mV in the mutant strain. This change in the driving force of electron transfer through the membrane was reflected in an inability of the mutant strain to accumulate a large transmembrane electrical potential on successive flashes.

Cytochrome *bc* complexes are membrane protein complexes found in almost every energy transducing membrane. The two major subgroups best characterized are ubiquinol/cytochrome *c* oxidoreductase (also called complex III or the bc_1 complex[1]) and plastoquinol/plastocyanin oxidoreductase (or the $b_6 f$ complex) (*1*). The complexes share a number of structural and functional similarities, but there are conspicuous differences in the organization of cytochrome *b*. Whereas cyt bc_1 complexes contain a long cyt *b* which consists of a single polypeptide with 8 transmembrane helices associated with two *b*-hemes, cyt $b_6 f$ complexes contain two polypeptides, a short cyt *b* providing the ligands for the two cofactors (cyt b_6) and a small subunit called subunit IV. These two subunits are homologous respectively to the amino- and carboxy-terminal parts of the bc_1 complex protein. These two complexes present distinguishable characteristics in terms of the spectral and redox properties of the *b*-hemes, the inhibitor sensitivity of the quinone binding sites, or the functional behavior in some of the catalytic steps (*2*, *3*). However, it has been difficult to explain these features by this difference in the structural organization of the cyt *b*-part. In addition of the organization of the *b*-part of these complexes, another characteristic that has often been invoked to explain some of these differences is that the two histidines on helix D, ligands to the two *b*-hemes, are separated by 14 residues in cyt b_6 and 13 in cyt *b* (*4*, *5*). The additional residue is a highly conserved threonine found in every sequence of chloroplast or cyanobacterial cyt b_6. Analysis of protein databases revealed that short *b*-type cytochromes may also contain valine instead of threonine at this position, as is the case in firmicutes such as *Bacillus stearothermophilus* and *Bacillus subtilis*. The recently reported sequences of a long cyt b from *Chlorobium* and *Aquifex* also contain a valine at this position (see Figure 1). Interestingly, neither a long cyt *b* sequence containing an additional threonine nor a short cyt *b* sequence with only 13 residues between the two heme ligands in helix D has been reported so far. To determine how these features would affect the properties of the enzyme, we introduced each into the cyt *b* of *Rhodobacter sphaeroides*. This bacterium contains a bc_1 complex composed of four subunits. The three redox-containing proteins, cyt *b*, cyt c_1, and Rieske ISP, are highly homologous to their mitochondrial counterparts, whereas the fourth one, subunit IV, is specific to this bacterium (*6*). Surprisingly, an additional residue in helix D did not prevent the assembly of the bc_1 complex, and although it changed the properties

† This work was supported by NIH Grant GM35438.

‡ Department of Microbiology.

§ Center for Biophysics and Computational Biology.

[1] Abbreviations: bc_1 complex, ubiquinol/cytochrome c_2 oxidoreductase; $b_6 f$ complex, plastoquinol/plastocyanin oxidoreductase; cyt, cytochrome; DMSO, dimethyl sulfoxide; DTT, dithiothreitol; *E. coli*, *Escherichia coli*; EDTA, ethylenediaminetetraacetic acid; E_m, redox midpoint potential; MOPS, 3-(*N*-Morpholino)propanesulfonic acid; PCR, polymerase chain reaction; Q, ubiquinone or quinone; QH_2, ubihydroquinone or quinol; Q_i site, quinone reducing site; Q_o site, quinol oxidizing site; RC, reaction center; SDS−PAGE, sodium dodecyl sulfate−polyacrylamide gel electrophoresis; WT, wild type.

10.1021/bi9813476 CCC: $15.00
Published on Web 10/29/1998

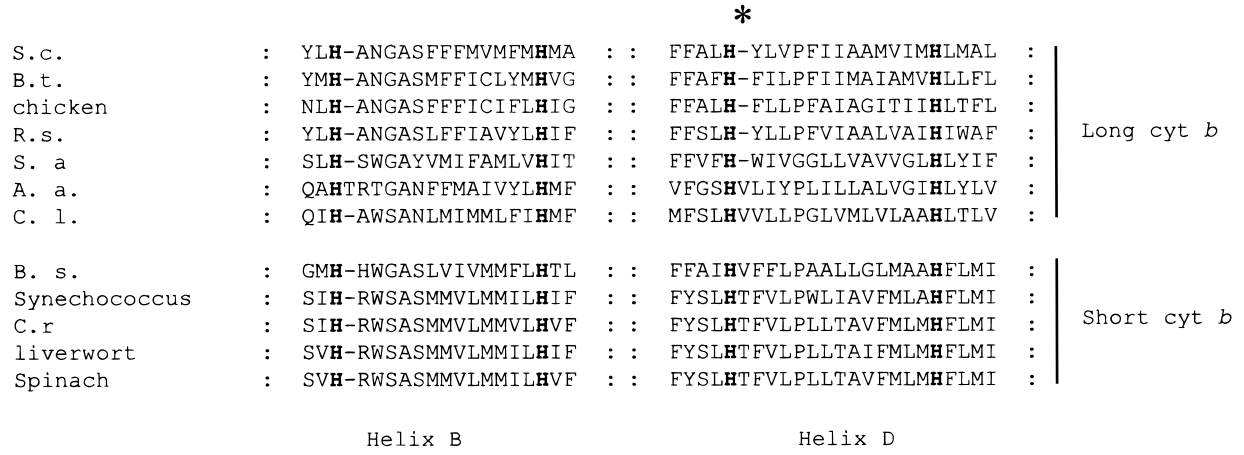

FIGURE 1: Multiple sequence alignment of the two heme binding helices of cyt *b*. The histidines, heme axial ligands, are shown in bold. The asterisk denotes the position of the additional residue in helix D. Long cyt *b* refers to the organization of the cyt *b* part of the complex as a single polypeptide. Long cyt *b* proteins are from mitochondria, *Saccharomyces cerevisae* (S. c.) (*47*), *Bos taurus* (B. t.), (*48*), and *Galus galus* (chicken) (*49*), or bacteria *Rhodobacter sphaeroides* (R. s.) (*7*), *Sulfolobus acidocaldarius* (S. a.) (*50*), *Aquifex aeolicus* (A. a.) (*51*); and *Chlorobium limicola* (C. l.) (*52*). Short cyt *b* refers to the organization of the cyt *b* part of the complex as two polypeptides from which the first contains 4 transmembrane helices. Short cyt *b* proteins are from bacteria, *Bacillus stearothermophilus* (B. s.) (*53*) and *Synechococcus PCC7002* (synechococcus) (*54*), or chloroplast, *Chlamydomonas reinhardtii* (C. r.) (*56*), *Marchantia polymorpha* (liverwort) (*57*), and *Spinacia oleracea* (spinach) (*58*).

of one of the *b*-hemes, the function of the complex was largely unaffected. In the strain with a split cyt *b*, some features specific for $b_6 f$ complexes were introduced, suggesting a role for the continuity in the span between helices D and E in determining the properties of the Q_i site. Our results are discussed in terms of the structural plasticity of cyt *b*.

MATERIALS AND METHODS

Bacteria Strains and Growth. Escherichia coli strains were grown in LB medium at 37 °C. Plasmids and their derivatives were maintained in *E. coli* strain JM109 in the presence of ampicillin (100 μg/mL) or tetracycline (10 μg/mL). *Rb. sphaeroides* were grown photosynthetically or aerobically in Sistrom medium at 30 °C. This media was supplemented with tetracycline (2 μg/mL) and kanamycin (20 μg/mL) for strains containing pRK415 derivatives (*7*).

Molecular Biology Techniques. All restriction endonucleases and polymerases were obtained from New England Biolabs. Synthetic primers for DNA mutagenesis were synthesized at the Biotechnology Center of the University of Illinois.

Site-directed mutagenesis was performed using PCR methods. The amplification was achieved with Deep $Vent_R$ DNA polymerase. The conditions described by the manufacturer were modified to include 10% (v/v) DMSO. PCR reactions were carried out using plasmid pGBM as a template. This plasmid was derived from pBC9 (*7*) by introducing thirteen neutral and unique restriction sites throughout the whole *fbc* operon, thus making it more suitable for in vitro manipulation. The modified operon was able to restore the WT properties of BC17, a strain of *Rb. sphaeroides* bearing a deletion of the whole *fbc* operon (*7*), to the same extent as its pBC9 counterpart. Details of the molecular engineering will be described elsewhere.

Construction of the Mutants. To construct the mutant 199T, two inserts 199TUP and 199TDOWN were generated by PCR amplification. The insert 199TUP was made with the following primers: start primer (p1), 5′CGGGATCCAGCTACAAGGCGCCTCGAGAGGTC3′; and end primer (p2), 5′GGAATTCAGG**TACGTA**TGCAGCGAGAAGAACCG3′. The insert 199TDOWN was made with the following primers: start primer (p3), 5′CGGGATCCGCA**TACGTA**CCTGCTGCCCTTCGTG3′; and end primer (p4), 5′GGAATTCGATGGCGAAGAACACTAGTAGGAC3′. Primers p2 and p3 contain an overlapping sequence which encompasses the inserted threonine codon (underlined) linked to a *Sna*BI restriction site (shown in bold). The two PCR products were digested by *Eco*RI and *Bam*HI and cloned into the *Eco*RI−*Bam*HI sites of pUC19. Standard recombinant DNA techniques were used first to fuse the two fragments using the *Sna*BI site and then to replace the *Xho*I−*Spe*I fragment of pGBM with the *Xho*I−*Spe*I fusion product leading to pBM199T.

The same strategy was used to construct the *Bsp*l mutant. Insert *Bsp*lUP was made using as start primer (p5), 5′-CGGGATCCATCGGCCATTCGATCCAGACCTGG3′, and as end primer (p6), 5′GGAATTC*TTA***CGTA**GGGTTGTTGTTGCCCGTCGA3′. Insert *Bsp*lDOWN was made using as start primer (p7), 5′CGGGATCC**TACG***TA*AGGAACACGCCATGGGCGTCGAAGTGCGCCGC3′, and as end primer (p8), 5′GGAATTCCTGTACAACCCAGACGTCGGCGGT3′. Primers p5 and p6 contain the overlapping restriction site *Sna*BI (shown in bold). The sequence inserted to split cyt *b* is underlined and is identical to the noncoding sequence found between the *fbc*F and *fbc*B ORFs. This sequence contains a stop codon (shown in italic), elements necessary to reinitiate the translation and the ATG codon. The inserts *Bsp*lUP and *Bsp*lDOWN were fused using the *Sna*BI site. The *Age*I−*Bsr*GI fragment of pGBM was replaced with the *Age*I−*Bsr*GI digestion product of the fused fragment, leading to pFBCSPL.

The two mutant *fbc* operons were subcloned into pRK415-1 and introduced into *Rb. sphaeroides* by conjugation with *E. coli* strain S17-1 (*7*).

Biochemical Methods. Chromatophores were isolated as described in Bowyer et al. (*8*). Protein determinations were made according to the method of Lowry modified by

Peterson (*9*) (Sigma, protein assay kit). SDS−PAGE analysis was carried out in a SDS−12.5% polyacrylamide gel (SDS−polyacrylamide gel system, Gibco BRL Life Technologies, Gaithersburg, MD) with a running buffer containing 49 mM Tris, 384 mM glycine, and 0.1% (w/v) SDS, pH 8.5. Coomassie blue staining was used for detection of the polypeptides. For immunodetection, chromatophores were solubilized in 1% SDS in the presence of 0.5 M DTT/Na_2CO_3. Proteins were separated on 15% precast gels for polyacrylamide electrophoresis (Bio-Rad Laboratories, Hercules, CA) with the same running buffer as above and electroblotted onto nitrocellulose sheets. Immunodetection was carried out using an enhanced chemiluminescence (ECL) method (Amersham Life Sciences Inc., Arlington Heights, IL) according to the specifications of the manufacturer. The bc_1 complex antiserum was prepared against a purified bc_1 complex from *Rb. sphaeroides* by the Biotechnology Center of the University of Illinois at Urbana-Champaign.

Biophysical Methods. The kinetics of flash-induced absorbance changes of the bc_1 complex and the reaction center were monitored on a single-beam spectrophotometer as described in Crofts and Wang (*9*). Optical redox titrations were performed as follows. Absorbance spectra of chromatophore preparations were recorded approximately every 10 mV, over a range of 400 mV, between −150 and 250 mV. The potential was modified by addition of either dithionite or ferricyanide, followed by a 3−5 min equilibration time. Titration curves were obtained from these data by abstracting values at appropriate wavelength pairs for the *b*-type cytochromes of each strain. The curves were fitted with either 2 or 3 Nernst components using the built-in nonlinear square fitting algorithm of the data analysis program Origin 4.0 (Microcal Software, Inc., Northampton, MA).

RESULTS

Modifications of Cytochrome b to Introduce b_6f-like Features Yielded Complexes that Still Allowed Photosynthetic Growth of the Site-Directed Mutants. Two separate modifications have been introduced in the cyt *b* of the purple bacterium *Rb. sphaeroides*. The first one was to insert in the helix D an additional threonine at position 199 (numbering according to the *Rb. Sphaeroides* sequence), next to the histidine 198 that provides a ligand to heme b_L. This introduces a residue which is present in all sequences for plant-type cyt b_6 sequences, but is missing from mitochondrial and purple bacterial cyt *b* sequences (Figure 1). This residue appears to be especially important because of its location in the α-helical span separating the two histidines that provide ligands to hemes b_L and b_H. Under photosynthetic growth conditions, where *Rb. sphaeroides* grows using cyclic electron transfer between the reaction center and the bc_1 complex, the mutant strain (strain 199T) had a generation time of 8 h, identical to the WT strain grown in the same conditions.

The second modification, characteristic of b_6f complexes and *bc* complexes from firmicutes, consisted of splitting the cyt *b* into two polypeptides. To mimic this effect, a sequence incorporating a stop codon, followed by signals allowing reinitiation of translation, was introduced in the region

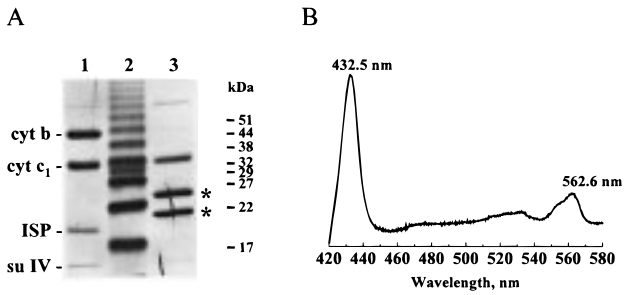

FIGURE 2: Purified bc_1 complex from *Bsp*l strain. A tag consisting of 6 histidines, attached at the carboxy-terminal part of cyt *b* of either the WT or the *Bsp*l strain was used to purify the bc_1 complex on a Ni−NTA affinity column. (A) Comparison of the polypeptide composition of bc_1 complexes isolated from the WT (lane 1) and the *Bsp*l strain (lane 3). Proteins were separated in a SDS−12.5% polyacrylamide gel and stained using Coomassie blue. Lane 2 shows the molecular weight ladder (Prestained Protein Ladder (6−60 kDa), Gibco BRL); the molecular weights of the standards are indicated on the right. The positions of the two bands corresponding to the split cyt *b* are shown with asterisks. (B) Dithionite reduced minus air-oxidized spectrum of the complex purified from the *Bsp*l strain.

encoding the loop connecting D and E transmembrane helices of cyt *b*. Thus the first polypeptide of the split cyt *b* mimics cyt b_6 and terminates at the sequence $G_{220}NNNPT_{225}$, while the second polypeptide would correspond to the b_6f-type subunit IV and starts with the sequence $MG_{226}VEVR_{230}$. When a histidine tag was added to the end of the second polypeptide of the split cyt *b*, a bc_1 subcomplex could be readily isolated and purified. The mutant complex no longer showed the 41 kDa band of the wild-type cyt *b* but instead had two new bands with apparent molecular weights of 23 and 20 kDa (Figure 2A, lane 3). From the spectrum of the preparation (see Figure 2B), showing that the purified complex retained the full complement of cytochromes, we can assume that one of the two bands corresponds to the first polypeptide of the split cyt *b* containing the two *b*-hemes, whereas the second one corresponds to the second, his-tagged polypeptide, equivalent to subunit IV of the b_6f complex. The apparent molecular weights of these bands are slightly lower than the values calculated from their predicted polypeptide sequences (25.2 and 25.9 kDa, respectively, for the first and second polypeptides). However, the abnormal electrophoretic migration of highly hydrophobic proteins often gives an underestimated molecular weight using SDS−PAGE. This has already been reported for cyt *b* in *Rb. sphaeroides* which shows an electrophoretic mobility of 40 kDa, whereas the molecular weight estimated from polypeptide sequence is 51 kDa (*6*). Taking this into account, we cannot assign the two bands specifically to the first or second polypeptide. It should be noted that the bc_1 complex from this strain presented different solubilization properties as compared to the WT. The purification procedure leading to an active bc_1 complex with all four subunits in the WT (Figure 2A, lane 1) (Guergova-Kuras, M. et al. (submitted for publication) gave a subcomplex which had lost the ISP and part of the native subunit IV when used with the modified bc_1 complex (Figure 2A, lane 3). Further work to optimize the purification procedure of the modified bc_1 complex is under way and will be reported elsewhere. Although this mutant (*Bsp*l) is able to grow photosynthetically (with a generation time of 10 h, as compared to 8 h for the WT), the culture after inoculation had to be preincubated in the absence of light for 24 h prior to being

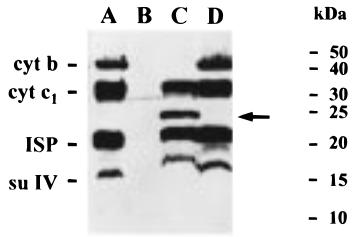

FIGURE 3: Immunoblot of chromatophore proteins. Polypeptides from WT (lane A), BC17 (lane B), *Bsp*l (lane C), and 199T (lane D) chromatophores. Proteins were separated by SDS−PAGE, electroblotted onto nitrocellulose, and reacted with an antiserum against the bc_1 complex. A molecular weight scale is given at the right side of the figure.

placed under photosynthetic conditions. This behavior suggests a possible sensitivity toward oxygen in the presence of light, but this issue was not further investigated.

Accumulation of the bc_1 Complex Subunits in the Mutant Strains. Using an antiserum directed against the bc_1 complex subunits of *Rb. sphaoeroides*, we investigated the accumulation of the subunits in membranes of the mutant strains. As shown on Figure 3 the immunoserum detects specifically the four polypeptides of the bc_1 complex (compare lanes A and B). It is interesting to note that in the strain BC17 (lane B), containing a deletion of the *fbc* operon (encoding the Rieske ISP, cyt *b* and cyt c_1), the native subunit IV encoded elsewhere in the genome (*11*) also failed to accumulate. Such an effect, where the absence of at least one subunit of a multimeric protein complex prevents the accumulation of other subunits of the same complex but from different transcriptional units, has been observed for various membrane protein complexes (*12*−*15*). In strain 199T (lane D) all four subunits of the bc_1 complex were accumulated at levels similar to that of the WT. The relative accumulation of cyt c_1, Rieske ISP, and subunit IV in *Bsp*l mutant (lane C) followed the same pattern as that of the WT. As expected, the full-length cyt *b* was not detected in this strain but a new band with an apparent molecular weight of ∼24 kDa (shown with an arrow on Figure 3) appeared with an intensity similar to that of the WT cyt *b* band, indicating that the antigenic epitope(s) recognized by the immunoserum is (are) located on one of the two parts of the split cyt *b*. We can therefore conclude that the neither the additional residue in cyt b of 199T strain nor the split in cyt b of *Bsp*l impairs the accumulation of the other subunits of the bc_1 complex.

Redox Properties of Cytochrome b in the Mutant Strains. Redox titrations aimed at a determination of the midpoint potentials of the *b*-hemes in the mutant and wild-type (WT) strains were performed at pH 7.0, as described in Materials and Methods. In both mutant strains, the midpoint potential of cyt b_H was almost unchanged, with a value of 50 ± 5 mV in both the WT and 199T, and a slightly increased value of 59 ± 10 mV in the *Bsp*l strain. In contrast, in both mutant strains, the redox properties of cyt b_L appeared to be altered. Whereas the cyt b_L potential is −90 mV in the WT strain, our results show that the split in cyt *b* (strain *Bsp*l) induced an increase of 50 mV in its potential, shifting it to −42 ± 12 mV. The change was even more dramatic with the additional threonine in the close vicinity of the heme. Cyt b_L of the 199T strain shows a midpoint potential of −5 ± 5 mV, representing a shift of 80 mV from the WT. Interestingly, both modifications increased the midpoint potential

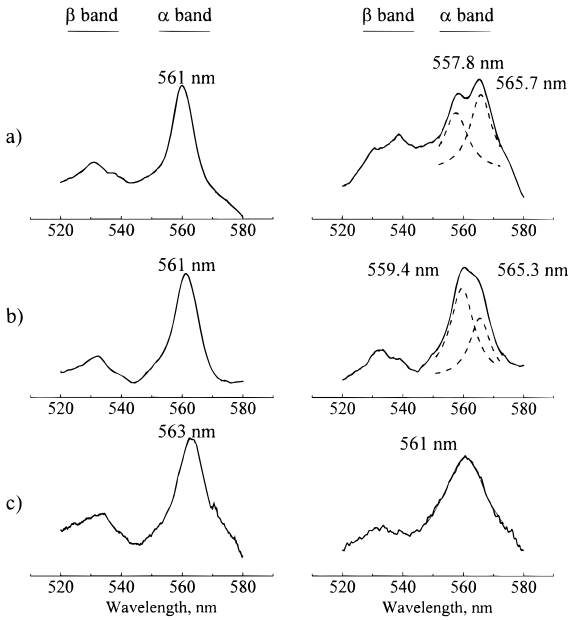

FIGURE 4: Absorption spectra of the *b* cytochromes in the mutant and WT strains. The left and right parts correspond, respectively, to the cyt b_H and cyt b_L spectra of bc_1 complex from (a) WT, (b) 199T, and (c) *Bsp*l strains. The difference spectra of the separate components from the redox titrations were determined as differences between spectra obtained at potentials separating a range where only one redox species was titrating. The positions of the peaks were determined using a Lorentzian deconvolution of the α-band region with either one (for cyt b_H of all strains and cyt b_L of the *Bsp*l strain) or two components (for cyt b_L of WT and 199T strains). The approximate region of the α and *β* bands are indicated on the top of the figure. Dashed lanes show the deconvoluted spectra for the transitions in the α band.

of cyt b_L, whereas the chloroplast cyt b_Ls are characterized with a midpoint potential of −140 to −150 mV (for a review, see ref *2*). An additional component which titrates around 150 mV and peaks at 561 nm was also observed in the titrations of both the WT and 199T strains. Its antimycin sensitivity allowed us to identify it as the previously described cyt b_{150} (*10*). Interestingly, this component, which results from the interaction of the b_H-heme with a quinol molecule at the Q_i site of the bc_1 complex (*16*−*18*), was not found in the *Bsp*l mutant. As this interaction was proposed to occur through the formation of a ferrocyt b_H/semiquinone complex at the Q_i site (*19*), we may conclude that the equilibrium between the quinol and the b_H-heme at this site as observed in the WT is modified in the *Bsp*l mutant.

Some Spectral Characteristics of b_6f Complexes Are Found in the Mutant bc_1 Complexes. The optical spectra of the *b*-cytochromes have been determined from the redox titration technique (20) and are shown on Figure 4. Our results show that the introduction of the additional threonine (199T mutant) modifies specifically the spectrum of cyt b_L, without affecting the optical properties of cyt b_H, which showed both the same peak (561 nm) and full width at half-height for its α-band (8 nm). A more detailed analysis of the cyt b_L spectra in the WT and 199T was made to deconvolute the components in the α- and *β*-bands. Four Lorentzian components were used, two for the α-band and two for the *β*-band. Since neither the potential nor the position of the bands was altered in the cyt b_H of 199T as compared to the WT, we assumed that the extinction coefficient for this heme was not modified by the mutation.

Table 1: Spectral Components of the α and *β* Bands of cyt b_L in Chromatophores of WT and 199T Strains

	Cyt b_L α band				Cyt b_L α band			
	peak 1 (nm)	area 1	peak 2 (nm)	area 2	peak 1 (nm)	area 1	peak 2 (nm)	area 2
WT	557.8	0.176	565.7	0.241	530.9	0.073	538.1	0.026
199T	559.4	0.194	565.3	0.157	532.2	0.043	538.2	0.008

[a] Conditions are as on Figure 4.

This allowed us to use the peak area of cyt b_H to normalize and compare the peak area for the deconvoluted components of cyt b_L. The results are summarized in Table 1. It is clear that the relative amplitudes of the low- and high-energy transitions in the α-band were changed in the 199T mutant. Whereas both the amplitude and the area of the lower-energy transition are the dominant components of the α-band in the WT, this transition became the minor component in the mutant. The ratio between the peak area of the high- and the low-energy transitions is 1:1.36 in the WT and 1:0.8 in the 199T mutant. Moreover, the splitting of this band, characteristic of the cyt b_L in the cyt bc_1 complex, is significantly decreased, mainly due to a 2 nm red shift of the higher-energy transition. The same 2 nm shift is also observed for the higher-energy vibrionic transition in the *β*-band. In the *β*-band, we also observed a change in the relative amplitude of the 2 transitions, although not as significant as in the α-band. The modifications in the optical spectra of the two *b*-type hemes in the *Bsp*l mutant are much more dramatic. The α-band of cyt b_L is no longer split and presents a single peak at 561 nm. The full width at half-height value of the α-band of the cyt b_H is slightly higher (10 nm), and the position of the peak at 563 nm represents a 2 nm red shift as compared to the WT. As a consequence, the optical properties of the *b*-hemes in this mutant appear very similar to those reported for the b_6-hemes. In all reported studies, the α band of a chloroplast-type cyt b_L presents a single peak and the α-band maxima of the two *b*-hemes appear almost undistinguishable (*2*, *3*).

Electrogenicity of the Mutant cyt bc₁ Complexes. Electrogenic events across the chromatophore membranes of *Rb. sphaeroides* can be monitored by measuring kinetic changes at 503 nm which reflect the "membrane voltmeter" provided by the electrochromic carotenoid bandshift (*21*). The kinetics can be separated into three phases. Phases I and II occur in the microsecond time scale and are associated with charge separation in the reaction center. Phase III (also called the slow phase), which occurs in the millisecond time scale, reflects electrogenic events in the cyt bc_1 complex and is completely inhibited by myxothiazol. Part of this phase, about 20%, is antimycin insensitive and has been shown to reflect the electron transfer from cyt b_L to cyt b_H (*21*). Figure 5 shows traces taken at 100 mV after one flash in both the WT (panel A) and the mutant strains 199T (panel B) and *Bsp*l (panel C). The slow phase in both 199T and *Bsp*l showed inhibitor sensitivity toward antimycin (traces b) and myxothiazol (traces c) at concentrations sufficient to inhibit the WT. It should be noted that antimycin and myxothiazol, which are inhibitors, respectively, of the Q_i and Q_o sites, are very efficient inhibitors when used on the bc_1 complex but have virtually no effect on the $b_6 f$ complex (*2*, *22*). Our results indicate that the split of cyt *b* or the additional residue

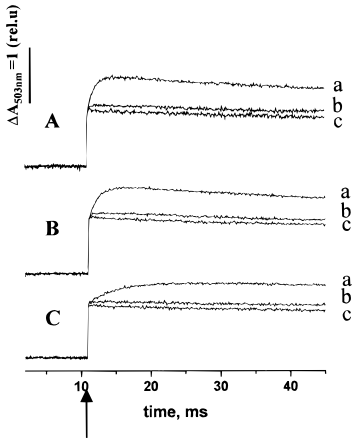

FIGURE 5: Effect of antimycin and myxothiazol on the electrochromic change. Electrochromic changes after a single saturating flash (indicated by an arrow) were measured at 503 nm in chromatophores from the WT (panel A), 199T (panel B), and *Bsp*l (panel C) strains. Chromatophores were resuspended at 0.3 μM RC for the WT and 199T and at 0.5 μM RC for *Bsp*l in 50 mM MOPS, pH 7.0, 100 mM KCl. Anaerobiosis was achieved with a constant argon flow. The redox potential in the cuvette was maintained at 100 mV. The following redox mediators were present: 2,3,5,6-tetramethyl-*p*-phenylenediamine (2 μM), 1,2-naphthoquinone (20 μM), 1,4-naphthoquinone (20 μM), phenazine methosulfate (1 μM), pyocyanine (1 μM), and Fe(III)Na EDTA (40 μM). Traces were normalized for the amplitude of the fast phase at 150 μs after the flash. Traces (a) were taken with no inhibitor added, traces (b), after addition of 3 μM antimycin, and traces (c), after addition of 5 μM myxothiazol.

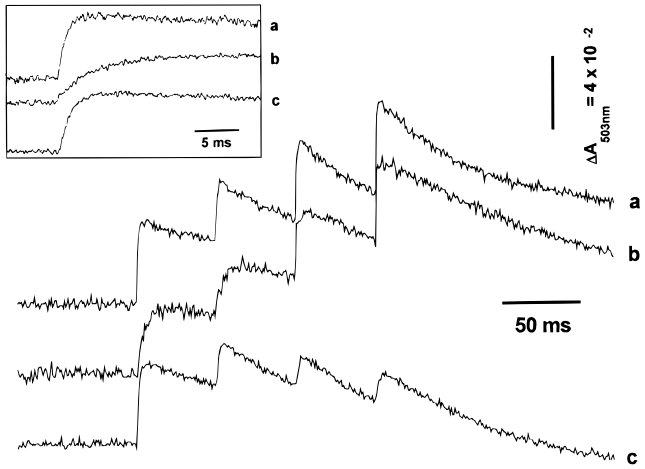

FIGURE 6: Kinetics of the slow phase. Experimental conditions as on Figure 5 traces, recorded in the presence of both antimycin (3 μM) and myxothiazol (5 μM), were subtracted from traces recorded when no inhibitors were present. Flashes were separated by 32 ms. The amplitudes were normalized for the amplitude of the fast phase (see Figure 5). The inset shows the slow phase after the first flash with a better time resolution: trace a, WT; trace b, *Bsp*l; and trace c, 199T.

in helix D is not the main determinant for the resistance of the $b_6 f$ complex toward these two inhibitors, contrary to what has often been suggested (*2*, *5*, *22*). The slow phase of the electrochromic shift for the two mutant strains is compared to that of the WT on Figure 6. Four consecutive flashes separated by 32 ms were given in order to follow the build-up of the transmembrane potential and the effects on turnover of the bc_1 complex in the different strains. In the 199T strain (trace c), one flash was sufficient to saturate the final level of transmembrane potential whereas in the wild type (trace

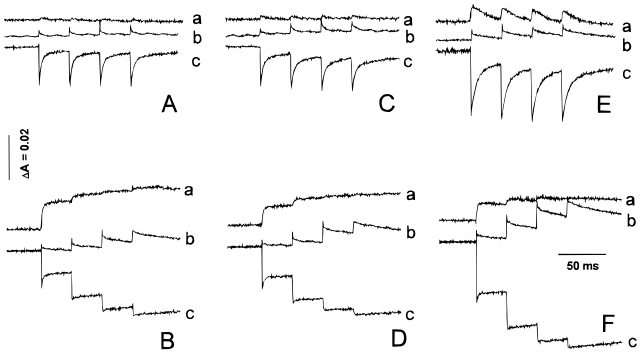

FIGURE 7: Kinetics of electron transfer. Kinetics were measured for cyt *b* (traces a), RC (traces b), and cyt c_1 plus cyt c_2 (cyt c_{total}) (traces c) for the WT (panels A and B), 199T (panels C and D), and *Bsp*I (panels E and F). For panels A, C, and E, chromatophore suspensions (in 50 mM MOPS pH 7.0, 100 mM KCl) at concentrations of RC as on Figure 5 were preincubated in the dark under anaerobic conditions, with the preparation poised at 100 mV ambient redox potential. Gramicidin (2 μg/mL) and 1 μM valinomycin were added to collapse the transmembrane electrochemical potential. Redox mediators were added as follows: 2,3,5,6-tetramethyl-*p*-phenylenediamine (2 μM), 1,2-naphthoquinone (10 μM), 1,4-naphthoquinone (10 μM), 1,2-naphthoquinone-4-sulfonic acid (10 μM), phenazine methosulfate (1 μM), pyocyanine (1 μM), and Fe(III)Na EDTA (50 μM). For panels B, D, and F, same conditions but in the presence of 3 μM antimycin. Kinetic traces were recorded after each of a series of four saturating flashes, separated by a time interval of 32 ms. Detection wavelengths were 542 nm for the RC, 551−542 nm for cyt c_{total}, and 561−569 nm for cyt *b*.

a) and the *Bsp*I mutant (trace b), saturation was not achieved even after four flashes. The inability of the 199T mutant to generate the same $\Delta\Psi$ as the WT is probably related to the smaller ΔE between the two *b*-hemes observed in this mutant (see above). After the first flash (see inset on Figure 6), the 199T mutant displayed no significant difference as compared to the WT, either in the overall cyt bc_1 complex turnover (traces c and a, respectively) or in the electron transfer between hemes b_L and b_H (not shown). On the other hand, the *Bsp*I mutant showed a slower turnover of the complex (trace b). However, the antimycin insensitive part was identical to the WT (not shown), suggesting that the electron transfer between the hemes was not affected by the mutation.

Electron Transfer through the Mutant bc_1 Complex is Altered but Not Impaired. The effects of the mutations on the electron transfer through the photosynthetic chain are shown on Figure 7. The initial redox state of the components in the electron-transfer chain was determined by poising the ambient redox potential at either 100 mV (Figure 7) or 200 mV (not shown). Under these conditions, the ubiquinone pool ($E_m{}^0{}_{(Q/QH2)} = 90$ mV) is respectively 30% reduced or fully oxidized. In both cases, the high-potential chain is in a reduced state whereas the low-potential *b*-heme chain is oxidized. Upon flash excitation in the presence of antimycin, the cyt b_H heme represents a single oxidizing equivalent, and a single turnover of the Q_o site of the complex completes its reduction. At 100 mV, the rate of cyt *b* reduction therefore reflects oxidation of one quinol at the Q_o site, which is the rate-limiting step. Figure 7 shows that the rates of cyt *b* reduction in the WT and in both mutant strains are similar. The half-time of cyt *b* reduction after the first flash is about 1.1−1.5 ms at 100 mV (traces a on panels B, D and F) and 5 ms at 200 mV (not shown) in all strains. This indicates that none of the kinetic parameters affecting the quinol oxidation at the Q_o site are significantly modified by the mutations. Additionally, the kinetics of cyt c_{total} are also similar in the mutants and the WT at both ambient potentials, suggesting that the electron transfer through the high-potential chain was not altered either (compare traces c on panels B, D, and F). In the absence of inhibitor we observe a normal turnover of the bc_1 complex in 199T as shown on panel C (compare with panel A, showing the WT). Since the rates of reduction and oxidation of cyt *b* are similar, no net change in the absorption of cyt *b* is observed (traces a on panels A and C). By contrast the *Bsp*I mutant presents a decrease in the overall turnover of the bc_1 complex (compare panel E with panel A), which is in agreement with the slower phase III in this mutant. In this strain, cyt *b* is completely reduced before its reoxidation occurs (compare the amplitude of cyt *b* reduction after the first flash in traces a of panels E and F). These results can be explained in terms of a modified equilibrium between the reduced cyt b_H and the semiquinone at the Q_i site and are discussed below.

DISCUSSION

Insertion of a Single Residue in a Membrane Helix of cyt b Does Not Impair Protein Folding or Assembly. The recently solved structures of cyt bc_1 complex (*23*, *24*) show a four helix bundle core formed by helices A, B, C, and D, tightly packed around two *b*-hemes. The two axial ligands for each heme are shared between helix B and D. On each helix the histidine residues providing the ligands are separated by 13 amino acids. In an α-helix with standard phi and psi angles, this would locate the ligands on the same side of the helix, with the two hemes approximately four turns apart. The introduction of a threonine residue in helix D, between the two histidines, would be expected to have consequences on the secondary structure, folding, and stability of the protein which would be reflected in the properties of the hemes and ultimately in the electron-transfer properties of the bc_1 complex. Our results show that the introduction of the additional threonine has a relatively minor effect, which appears to be limited to the properties of the heme b_L. The complex is assembled and fully functional. Therefore it appears that cyt *b* is able to accommodate the presence of the additional residue without any major change in the properties of the enzyme. Previous studies have shown that both soluble (*25*, *26*) and membrane proteins (*27*) can tolerate single amino acid insertions in α-helices with varying degrees of alteration in the activity and stability of the proteins. Crystallographic studies on insertion mutants of T4 lysozyme and staphylococcal nuclease identified two types of structural change that compensate the effect of the amino acid insertion. In the first, the additional residue is incorporated in the helical structure, and the wild-type residues are shifted one residue toward the end of the helix, thus displacing the effect of the insertion to a loop or a bend (*25*, *26*). In our case, since the insertion was introduced between the two histidine ligands on helix D, such a translocation would be expected to rotate by approximately 100° the position of one of the two ligands. Since the geometry of histidine side chains which are involved in the coordination of metal ions appears to be very constrained (*28*), such a rotation would be likely to impair the proper binding of the cofactors. In the second type of structural change, the additional residue is bulged or looped out of the

helix. The change is thus localized to the site of the insertion where the helical structure is disrupted. According to Vetter et al. (*25*), this type of reorganization would be less common because of the higher destabilization energy it involves. Nevertheless, we favor this type of reorganization as a possible mechanism by which cyt *b* deals with the insertion of the threonine residue. From electrospray mass spectrometry measurements on heme dissociation in cyt b_5, the average stabilization energy provided by the binding of a *b*-type heme in this four helix bundle protein was found to be around 100 kJ/mol (*29*). It has also been previously shown that the presence of the b_H-heme is not required for the proper folding and assembly of the cyt *b* within the bc_1 complex (*30*). We can thus speculate that the additional stabilization energy provided by the ligation of the b_H-heme could be used in the 199T mutant to bulge out the inserted residue. Indeed the destabilization in this type of reorganization for both T4 lysozyme and staphylococcal nuclease is not higher than 30 kJ/mol (*31*).

The Insertion of an Additional Residue in the D Helix of cyt b Has Only Minor Effects on the Function of the bc_1 Complex. The functional analogue of the bc_1 complex in chloroplast is the cyt b_6f complex. Although the two complexes are very similar in both their redox composition and their functional aspects, they differ in some important characteristics. Thus the presence of 13 residues separating the two His ligands in helix D of cyt *b*, instead of 14 residues in the cyt b_6, was proposed as the reason for the cyt b_L split α-band observed only with long cyt *b*. The additional threonine residue was also proposed to explain the lower midpoint potential of the *b*-hemes of cyt b_6 (*1*, *5*). Our results show that the insertion of the threonine in cyt *b* has only minor effects on the bc_1 complex. The properties of cyt b_L are indeed affected, but the midpoint potential is shifted to a more positive value. This effect cannot be accounted for by a simple change in the hydrophobicity of the heme environment, since the introduction of a polar residue has been shown to decrease the E_m value of the heme (*32*). However positive changes in heme potential have been reported upon modification of the hydrogen bonding either of the imidazole ligand (*33*) or of the propionates of the heme molecule (*34*). Another possible reason could be a change in the orientation of the imidazole ligand plane (*35*). Neither of these possibilities can be excluded as a mode of reorganization in the b_L-heme pocket due to the additional threonine.

One interesting consequence of the increase of the E_m value of the cyt b_L heme is the decrease in the driving force available for electron transfer across the membrane in the low-potential chain. This has a direct consequence in the ability of the bc_1 complex to drive electrons against the transmembrane potential, and this is reflected in the slow phase of the carotenoid shift of the 199T mutant, which is saturated after the first flash. This must to some extent reflect a kinetic impediment, since the overall driving force provided by the redox drop between quinol and cyt c_2 is the same. To provide the potential needed to reduce cyt b_H against a membrane potential of 200 mV, the cyt b_L in wild type is poised at ∼−90 mV, close to the midpoint (*36*). To achieve this poise in the mutant, the heme b_L would have to be ∼96.5% reduced, which would lower the kinetic concentration of the oxidized form available at the Q_o site.

Complementation of cyt b Fragments Allows the Assembly of a Functional bc_1 Complex. Reconstitution of functional proteins from independently synthesized fragments has been reported for several systems, from prokaryote to eukaryote organisms, for soluble and membrane proteins, both in vitro and in vivo (*37*−*40*). Here we show not only that cyt *b* can be reconstituted from two fragments but also that the "split" cyt *b* can be assembled into a functional hetero-oligomeric complex. In *Rb. sphaeroides*, the bc_1 complex is composed of four polypeptides, cyt *b*, cyt c_1, the Rieske iron−sulfur protein (ISP), and a small subunit called subunit IV, likely organized as a homodimer. Moreover, it has been previously shown that the presence of these four subunits is required for the formation of a fully active bc_1 complex (*41*). In this study, cyt *b*, which encompasses eight transmembrane helices numbered from A to H, was split in the span between helix D and E. It should be noted that the recently published structure of the bovine mitochondrial bc_1 complex (*23*) has indicated that the cyt *b* presents a two domain organization. The first domain encompasses helices A−E, whereas the second encompassed helices F, G, and H. Popot and Engelman proposed a two stage model for the assembly of membrane proteins, in which the transmembrane helices are formed independently and assemble later into a final tertiary structure (*42*). In this context, we can assume that the formation of the first domain (A−E) in our mutant would be impeded by the lack of helix E. On the other hand, the presence of this helix in the second fragment would facilitate the complementation between the two fragments by stabilizing the final structure only when helix E becomes a part of the first structural domain. Our results suggest that the complementation between the two fragments of the split cyt *b* allows a final conformation which is sufficiently close to the native one to allow rapid electron transfer through the mutant bc_1 complex. Indeed, previous mutagenesis works (for a review, see Brasseur et al. (*43*)) as well as the crystal structures of the bc_1 complex (*23*, *24*) have shown that residues from the two parts of the split cyt *b* contribute to the quinol oxidation (Q_o) and quinone reduction (Q_i) sites. In both of our mutants, the partial reactions occurring at the Q_o site are similar to the WT, and the mutant strains were still sensitive to specific inhibitors of both sites. This suggests that the structural configuration of the site is essentially the same as in the WT. The differences in the partial reactions occurring at the Q_i site observed in the *Bsp*l mutant are discussed below.

The Presence of the Split cyt b in the bc_1 Complex Confers Some Properties Similar to those of cyt b_6f Complexes. Although the modified Q-cycle has been widely accepted as a model for the operation of both the bc_1 and b_6f complexes, there are some differences concerning the details of the mechanism in each case (for a review, see Cramer et al. (*3*)), which can be accounted for in terms of the altered thermodynamic characteristics of the redox components, and changes in kinetic parameters. A major difference in behavior lies in the processes leading to the quinone reduction at the Q_i site. The reduction of the quinone at the Q_i site of the bc_1 complex occurs via the formation of a stable semiquinone after the first turnover of the Q_o site. In the b_6f complex, a stable semiquinone at the Q_i site has never been observed and it has been proposed that the two *b*-hemes must be consecutively reduced (two turnovers of the Q_o site)

before the reduction of the quinone takes place (*44*, *45*). Moreover antimycin which is a strong inhibitor of the Q_i site of the bc_1 complexes has no effect on the $b_6 f$ complexes. In the mutant bc_1 complex bearing the split cyt *b*, we retain the sensitivity to antimycin characteristic of the bc_1 complex (Figure 5). This is a good indication that the Q_i site, or at least the region involved in the binding of antimycin, adopts a conformation close to that of the native one. Interestingly, this mutation affects the formation of a stable semiquinone at this site. The cyt b_{150} component, which results from the interaction between cyt b_H and the semiquinone ($Q_i^{\bullet -}$) at this site, was not observed in the *Bsp*l mutant. Crofts et al. (*19*) have derived an expression describing the equilibrium constant for the reaction leading to the formation of the cyt b_{150} component. On binding of QH_2, one electron is transferred to the oxidized cyt b_H heme to produce a [cyt b_H^- $Q^-(2H^+)$] state, which is likely an intermediate in the forward reaction. Deconvolution of the equilibrium constant into its thermodynamic components shows that two factors contribute to the formation of the cyt b_{150} intermediate. At any defined pH, the equilibrium constant for formation of the [cyt b_H^- $Q^-(2H^+)$] intermediate (the cyt b_{150} form) is given by:

$$K_{eq} = \exp\{(E_{m(\text{cyt } b_H)} + E_{m(Q/QH^{\bullet})} - 2E_{m(Q_{pool})})F/RT)\}$$

where $E_{m(Q/QH^{\bullet})}$ refers to the bound couple, $E_{m(\text{cyt } b_H)}$ is the potential of the heme in the absence of interaction, and $E_{m(Q_{pool})}$ is the potential of the Q/QH_2 couple in the pool. The important factors in defining a value for K_{eq} are the E_m value for cyt b_H and the stability of the semiquinone, while the relative affinities of Q and QH_2 at the Q_i site determine the apparent midpoint of the cyt b_{150} form.

In the present experiments, since the E_m value for cyt b_H was unchanged, we would have to ascribe the loss of cyt b_{150} to a much less stable semiquinone at the Q_i site. This reduced stability of the semiquinone also provides a straightforward explanation for the altered kinetics of electron transfer from cyt b_H seen in *Bsp*l (Figure 7), since the redox potential of the acceptor couple $Q/Q^{\bullet -}$ would be lowered in this strain. Joliot and Joliot (*44*) and Kramer and Crofts (*45*) have previously suggested that the similar kinetic behavior seen in chloroplasts reflects an unstable semiquinone at the Q_i site of the $b_6 f$ complex.

We may note that, even if the split site has the same configuration as that of the wild-type complex, the introduction of two charged groups, represented by the C and N termini, will likely have a profound effect on the local electrostatic environment. Relatively modest mutational changes in this span produce effects on the turnover of the complex and the thermodynamic characteristics of the redox components (*19*, *46*), so this minimal perturbation consequent on the split may be sufficient to explain the effects observed.

ACKNOWLEDGMENT

We thank Prof. P. Joliot and Prof. S. Subramaniam for helpful discussions, Dr. F.-A. Wollman for critical reading of the manuscript, and Dr. D. Berthold for initiating the bc_1 complex antibodies project.

REFERENCES

1. Cramer, W. A., Black, M. T., Widger, W. R., and Girvin, M. E. (1987) in *The Light Reactions* (Barber, J., Ed.) pp 447−493, Elsevier Science Publishers, Amsterdam.
2. Kallas, T. (1994) in *The Molecular Biology of Cyanobacteria* (Bryant, D. A., Ed.) pp 259−317, Kluwer Academic Publishers, Dordrecht, The Netherlands.
3. Cramer, W. A., Soriano, G. M., Ponomarev, M., Huang, D., Zhang, H., Martinez, S. E., and Smith, J. L. (1996) *Annu. Rev. Plant Physiol. Plant Mol. Biol. 47*, 477−508.
4. Widger, W. R., Cramer, W. A., Herrmann, R. G., and Trebst, A. (1984) *Proc. Natl. Acad. Sci. U.S.A. 81*, 674−678.
5. Hauska, G., Nitschke, W., and Herrmann, R. G. (1988) *J. Bioenerg. Biomembr. 20*, 211−228.
6. Andrews, K. M., Crofts, A. R., and Gennis, R. B. (1990) *Biochemistry 29*, 2645−2651.
7. Yun, C. H., Beci, R., Crofts, A. R., Kaplan, S., and Gennis R. B. (1990) *Eur. J. Biochem. 194*, 399−411.
8. Bowyer, J. R., Meinhardt, S. W., Tierney, G. V., and Crofts, A. R. (1981) *Biochim. Biophys. Acta 635*, 167−186.
9. Peterson, G. L. (1977) *Anal. Biochem. 83*, 346−356.
10. Crofts, A. R., and Wang, Z. (1989) *Photosynth. Res. 22*, 69−87.
11. Usui, S., and Yu, L. (1991) *J. Biol. Chem. 266*, 15644−15649.
12. Crivellone, M. D., Wu, M., and Tzagoloff, A. (1988) *J. Biol. Chem. 263*, 14323−14333.
13. Kuchka, M. R., Mayfield, S. P., and Rochaix, J.-D. (1988) *EMBO J. 7*, 319−324.
14. de Vitry, C., Olive, J., Drapier, D., Recouvreur, M., and Wollman, F.-A. (1989) *J. Cell Biol. 109*, 991−1006.
15. Kuras, R., and Wollman, F.-A. (1994) *EMBO J. 13*, 1019−1027.
16. Salerno, J. C., Xu Y., Osgood, M. P., Kim, C. H., and King, T. E. (1989) *J. Biol. Chem. 264*, 15398−15403.
17. Glaser, E. G., Meinhardt, S. W., and Crofts, A. R. (1984) *FEBS Lett. 178*, 336−342.
18. Rich, P. R., Alan, E. J., Madgwick, S. A., and Moody, A. J. (1990) *Biochim. Biophys. Acta 1018*, 29−40.
19. Crofts, A. R., Barquera, B., Bechmann, G., Guergova, M., Salcedo-Hernandez, R., Hacker, B., Hong, S., and Gennis, R. B. (1995) in *Photosynthesis: from Light to Biosphere* (Mathis, P., Ed.) Vol. II, pp 493−500, Kluwer Academic Publishers, Dordrecht, The Netherlands.
20. Berry, E. A., Huang, L.-S., and DeRose, V. J. (1991) *J. Biol. Chem. 266*, 9064−9077.
21. Glaser, E. G., and Crofts, A. R. (1984) *Biochim. Biophys. Acta 766*, 322−333.
22. Frank, K., and Trebst, A. (1995) *Photochem. Photobiol. 61*, 2−9.
23. Xia, D., Yu, C.-A., Kim, H., Xia, J.-Z., Kachurin, A., Zhang L., Yu, L., and Deisenhofer, J. (1997) *Science 277*, 60−66.
24. Zhang, Z., Huang, L.-S., Shulmeister, V. M., Chi, Y.-I., Kim, K.-K., Hung, L.-W., Crofts, A. R., Berry, E. A., and Kim, S.-H. (1998) *Nature 392*, 677−684.
25. Vetter, I. R., Baase, W. A., Heinz, D., Xiong, J. P., Snow, S., and Matthews, B. W. (1996) *Protein Sci. 5*, 2399−2415.
26. Heinz, D. W., Baase, W. A., Dahlquist, F. W., and Matthews, B. W. (1993) *Nature 361*, 561−564.
27. Marti, T., Otto, H., Rosselet, S. G., Heyn, M. P., and Khorana, H. G. (1992) *Proc. Natl. Acad. Sci. U.S.A. 89*, 1219−1223.
28. Chakarabarti, P. (1990) *Protein Eng. 4*, 57−63.
29. Hunter, C. L., Mauk, A. G., and Douglas, D. J. (1997) *Biochemistry 36*, 1018−1025.
30. Yun, C. H., Crofts A. R., and Gennis, R. B. (1991) *Biochemistry 30*, 6747−6754.
31. Sondek, J., and Shortle, D. (1990) *Proteins 7*, 299−305.
32. Kassner, R. J. (1972) *Proc. Natl. Acad. Sci. U.S.A. 69*, 2263−2267.
33. O'Brien, P., and Sweigart, D. A. (1985) *Inorg. Chem. 24*, 1405−1409.
34. Cutler, R. L., Davies, A. M., Creighton, S., Warshel, A., Moore, G. R., Smith, M., and Mauk, A. G. (1989) *Biochemistry 28*, 3188−3197.
35. Safo, M. K., Gupta, G. P., Walker, F. A., and Scheidt, W. R. (1991) *J. Am. Chem. Soc. 113*, 5497−5500.

36. Chen, Y., and Crofts, A. R. (1990) in *Current Research in Photosynthesis* (Baltscheffsky, M., Ed.) Vol. III, pp 287−290, Kluwer Academic Publishers, Dordrecht, The Netherlands.
37. Bibi, E., and Kaback, H. R. (1990) *Proc. Natl. Acad. Sci. U.S.A. 87*, 4325−4329.
38. Kahn, T. W., and Engelman, D. M. (1992) *Biochemistry 31*, 6144−6151.
39. Koebnick, R. (1996) *EMBO J. 15*, 3529−3537.
40. Schmidt-Rose, T., and Jentsch, T. J. (1997) *J. Biol. Chem. 272*, 20515−20521.
41. Yu, L., and Yu, C. A. (1991) *Biochemistry 30*, 4934−4939.
42. Popot, J. L., and Engelman, D. M. (1990) *Biochemistry 29*, 4031−4037.
43. Brasseur, G., Saribas A. S., and Daldal F. (1996) *Biochim. Biophys. Acta 1275*, 61−69.
44. Joliot, P., and Joliot A. (1984) *Biochim. Biophys. Acta 765*, 210−218.
45. Kramer, D. M., and Crofts, A. R. (1992) in *Research in Photosynthesis* (Murata, N., Ed.) Vol. II, pp 491−494; Kluwer Academic Publishers, Dordrecht, The Netherlands.
46. Hacker, B., Barquera, B., Crofts, A. R., and Gennis, R. B. (1993) *Biochemistry 32*, 4403−4410.
47. Claros, M. G., Perea, J., Shu, Y., Samatey, F. A., Popot, J. L., and Jacq, C. (1995) *Eur. J. Biochem. 228*, 762−771.
48. Anderson, S., de Bruijn, M. H., Coulson, A. R., Eperon, I. C., Sanger, F., and Young, I. G. (1982) *J. Mol. Biol. 156*, 683−717.
49. Kornegay, J. R., Kocher, T. D., Williams, L. A., and Wilson, A. C. (1993) *J. Mol. Evol. 37*, 367−379.
50. Castresana, J., Lubben, M., and Saraste, M. (1995) *J. Mol. Biol. 250*, 202−210.
51. Deckert, G., Warren, P. V., Gaasterland, T., Young, W. G., Lenox, A. L., Graham, D. E., Overbeek, R., Snead, M. A., Keller, M., Aujay, M., Huber, R., Feldman, R. A., Short, J. M., Olson, G. J., and Swanson, R. V. (1998) *Nature 392*, 353−358.
52. Schuetz, M., Zirngibl, S., Le Coutre, J., Buettner, M., Xie, D.-L., Nelson, N., Deutzmann, R., and Hauska, G. (1994) *Photosynth. Res. 39*, 163−174.
53. Sone, N., Tsuchiya, N., Inoue, M., and Noguchi, S.(1996) *J. Biol. Chem. 271*, 12457−12462.
54. Brand, S. N., Tan, X., and Widger, W. R. (1992) *Plant Mol. Biol. 20*, 481−491.
55. Buschlen, S., Choquet, Y., Kuras, R., and Wollman, F. A. (1991) *FEBS Lett. 284*, 257−262.
56. Fukuzawa, H., Kohchi, T., Sano, T., Shirai, H., Umesono, K., Inokuchi, H., Ozeki, H., and Ohyama, K. (1988) *J. Mol. Biol. 203*, 333−351.
57. Westhoff, P., Farchaus, J. W., and Herrmann, R. G. (1986) *Curr. Genet. 11*, 165−169.

BI9813476